THE FUNDAMENTAL PLANE FOR $z = 0.8$–0.9 CLUSTER GALAXIES

INGER JØRGENSEN,[1] KRISTIN CHIBOUCAS,[1] KATHLEEN FLINT,[1,2] MARCEL BERGMANN,[3] JORDI BARR,[4] AND ROGER DAVIES[4]

ABSTRACT

We present the fundamental plane (FP) for 38 early-type galaxies in the two rich galaxy clusters RX J0152.7−1357 ($z = 0.83$) and RX J1226.9+3332 ($z = 0.89$), reaching a limiting magnitude of $M_B = -19.8$ in the rest frame of the clusters. While the zero-point offset of the FP for these high-redshift clusters relative to our low-redshift sample is consistent with passive evolution with a formation redshift of $z_{form} \approx 3.2$, the FP for the high-redshift clusters is not only shifted as expected for a mass-independent z_{form} but rotated relative to the low-redshift sample. Expressed as a relation between the galaxy masses and the mass-to-light ratios, the FP is significantly steeper for the high-redshift clusters than for our low-redshift sample. We interpret this as a mass dependency of the star formation history, as has been suggested by other recent studies. The low-mass galaxies ($10^{10.3}\ M_\odot$) have experienced star formation as recently as $z \approx 1.35$ (1.5 Gyr prior to their look-back time), while galaxies with masses larger than $10^{11.3}\ M_\odot$ had their last major star formation episode at $z > 4.5$.

Subject headings: galaxies: clusters: individual (RX J0152.7−1357, RX J1226.9+3332) —
galaxies: evolution — galaxies: stellar content

1. INTRODUCTION

The fundamental plane (FP) for elliptical (E) and lenticular (S0) galaxies is a key scaling relation, which relates the effective radii, the mean surface brightnesses, and the velocity dispersions in a relation that is linear in logarithmic space (e.g., Dressler et al. 1987; Djorgovski & Davis 1987; Jørgensen et al. 1996, hereafter JFK1996). The FP can be interpreted as a relation between the galaxy masses and their mass-to-light ratios (M/L). For low-redshift cluster galaxies, the FP has very low internal scatter (e.g., JFK1996). It is therefore a powerful tool for studying the evolution of the M/L as a function of redshift (e.g., Jørgensen et al. 1999; Kelson et al. 2000; van de Ven et al. 2003; Gebhardt et al. 2003; Wuyts et al. 2004; Treu et al. 2005; Ziegler et al. 2005). These authors all find that the FP at $z = 0.2$–1.0 is consistent with the passive evolution of the stellar populations of the galaxies, generally with a formation redshift $z_{form} > 2$. Most previous studies of the FP at $z = 0.2$–1.0 cover fairly small samples of galaxies in each cluster and are limited to a narrow range in luminosities, and therefore masses, making it very difficult to detect possible differences in the FP slope. A few recent studies indicated a steepening of the FP slope for $z \sim 1$ galaxies (di Serego Alighieri et al. 2005; van der Wel et al. 2005; Holden et al. 2005). These studies and the studies of the K-band luminosity function (Toft et al. 2004) and the red sequence (de Lucia et al. 2004) at $z \approx 0.8$–1.2 suggest a mass dependency of the formation epoch.

We present the FP for two galaxy clusters, RX J0152.7−1357 at $z = 0.83$ and RX J1226.9+3332 at $z = 0.89$. Our samples reach apparent i'-band magnitudes of 22.5–22.8, equivalent to an absolute magnitude of $M_B = -19.8$ in the rest frame of the clusters. No other published samples suitable for studies of the cluster galaxy FP at $z > 0.8$ go this deep. Our study of these two clusters is part of the Gemini/*HST* Galaxy Cluster Project,

[1] Gemini Observatory, 670 North A'ohoku Place, Hilo, HI 96720; ijorgensen@gemini.edu, kchibouc@gemini.edu.
[2] Current address: State University of New York at Stony Brook, The Reinvention Center, Stony Brook, NY 11794; kathleen.flint@stonybrook.edu.
[3] Gemini Observatory, Casilla 603, La Serena, Chile; mbergmann@gemini.edu.
[4] Department of Astrophysics, University of Oxford, Keble Road, Oxford OX1 3RH, UK; jmb@astro.ox.ac.uk, rld@astro.ox.ac.uk.

which is described in detail in Jørgensen et al. (2005). We adopt a ΛCDM cosmology with $H_0 = 70$ km s^{-1} Mpc^{-1}, $\Omega_M = 0.3$, and $\Omega_\Lambda = 0.7$.

2. OBSERVATIONAL DATA

Spectroscopy for RX J0152.7−1357 and RX J1226.9+3332 was obtained with the Gemini Multi-Object Spectrograph at Gemini North (GMOS-N; Hook et al. 2004). The data for RX J0152.7−1357 are published in Jørgensen et al. (2005). The reduction of the RX J1226.9+3332 spectroscopy was done using similar techniques, with suitable changes to take into account the use of the nod-and-shuffle mode of GMOS-N (I. Jørgensen et al. 2006, in preparation). We use *Hubble Space Telescope* (*HST*) archive data of the two clusters obtained with the Advanced Camera for Surveys (ACS). In this Letter we use effective radii, r_e, and mean surface brightnesses, $\langle I \rangle_e$, derived from either F775W or F814W observations, calibrated to the rest-frame B band (see K. Chiboucas et al. 2006, in preparation, for details). The GALFIT program (Peng et al. 2002) was used to determine r_e and $\langle I \rangle_e$. We fit the cluster members with Sérsic (1968) and $r^{1/4}$ profiles. The combination that enters the FP, $\log r_e + \beta \log \langle I \rangle_e$ ($\beta = 0.7$–0.8), differs very little for the two choices of profiles. In the following we use the parameters from $r^{1/4}$-fits for consistency with our low-redshift comparison data. None of the main conclusions of this Letter would change had we chosen to use the Sérsic fits. Masses of the galaxies are derived as $M = 5\sigma^2 r_e\ G^{-1}$.

Our Coma Cluster sample serves as the low-redshift reference sample (Jørgensen 1999). We have obtained new B-band photometry of this sample with the McDonald Observatory 0.8 m telescope and the Primary Focus Camera (Claver 1995). The data were reduced in a standard fashion, and effective parameters were derived as described in Jørgensen et al. (1995). Table 1 summarizes the sample sizes and some key cluster properties.

3. THE FUNDAMENTAL PLANE AT $z = 0.8$–0.9

We first establish the FP for the Coma Cluster data. In order to limit the effect of differences in sample selection for the Coma Cluster sample and the high-redshift sample, we exclude

TABLE 1
GALAXY CLUSTERS AND SAMPLES

Cluster	Redshift	$\sigma_{\mathrm{cluster}}$[a] (km s^{-1})	N_{galaxies}[b]	N_{analysis}[c]	Ref.
Coma = Abell 1656	0.024	1010	116	105	Jørgensen 1999
RX J0152.7−1357	0.835	1110	29	20	Jørgensen et al. 2005
RX J1226.7+3332	0.892	1270	25	18	This Letter

[a] Cluster velocity dispersion.
[b] Number of galaxies observed.
[c] Number of galaxies included in the analysis (see text).

galaxies with $M < 10^{10.3} M_\odot$ as well as emission-line galaxies. The sum of the absolute residuals perpendicular to the relation was minimized. We find

$$\log r_e = (1.30 \pm 0.08) \log \sigma - (0.82 \pm 0.03) \log \langle I \rangle_e - 0.443,$$
(1)

where r_e is the effective radius in kiloparsecs, σ is the velocity dispersion in kilometers per second, and $\langle I \rangle_e$ is the surface brightness within r_e in units of $L_\odot$ pc^{-2}. The uncertainties on the coefficients are determined using a bootstrap method (see JFK1996 for details). The rms of the fit is 0.08 in $\log r_e$. The coefficients are in agreement with other determinations available in the literature (e.g., JFK1996; Colless et al. 2001; Blakeslee et al. 2002; Bernardi et al. 2003).

Figure 1 shows the Coma Cluster FP face-on as well as two edge-on views of the relation, with the high-redshift sample overplotted. The FP for the high-redshift sample is not only offset from the Coma Cluster FP but appears "steeper." As there is no significant FP zero-point difference between the two high-redshift clusters, we treat the high-redshift galaxies as one sample. Deriving the FP for the high-redshift sample using the same technique and sample criteria as for the Coma Cluster, we find

$$\log r_e = (0.60 \pm 0.22) \log \sigma - (0.70 \pm 0.06) \log \langle I \rangle_e + 1.13,$$
(2)

with an rms of 0.09 in $\log r_e$. The difference in the coefficient for $\log \sigma$ between equations (1) and (2) is $\Delta \alpha = 0.70 \pm 0.23$, a 3 σ detection of a difference in the FP slope. The internal scatter of the two relations is similar. Figure 1d shows the FP as a relation between the galaxy masses and the M/L. The fit to the Coma sample, excluding the low-mass galaxies, gives

$$\log (M/L) = (0.24 \pm 0.03) \log M - 1.75,$$
(3)

with an rms of 0.09 in $\log (M/L)$. Fitting the high-redshift sample, using the same mass limit, gives

$$\log (M/L) = (0.54 \pm 0.08) \log M - 5.47,$$
(4)

with an rms of 0.14 in $\log (M/L)$. The internal scatter in $\log (M/L)$ is not significantly different for the two relations. We find 0.07 and 0.08 for the Coma sample and the high-redshift sample, respectively. Even with the same mass limit enforced on both samples, one might argue that the fits are still affected by the difference in the luminosity limit. Therefore, we also fit a subsample of the Coma sample limited at $M_B = -19.8$ mag. The coefficient for $\log M$ is in this case 0.28 ± 0.06. Thus, the difference between the coefficients for the high-redshift and low-redshift samples is at the 3 σ level.

4. POSSIBLE SYSTEMATIC EFFECTS

To test how well we recover input r_e, $\langle I \rangle_e$, and $\log r_e + \beta \log \langle I \rangle_e$ ($\beta = 0.7$–0.8), we simulate HST/ACS observations of galaxies with Sérsic profiles with $n = 0.8$–4.6 and effective parameters matching our Coma sample. For $n > 2$, the $r^{1/4}$-fits recover $\log r_e$ with an rms of 0.15. However, $\log r_e + \beta \log \langle I \rangle_e$ is recovered with an rms scatter of only ≈ 0.02 for β between 0.7 and 0.8. There are no systematic effects as a function of effective radii or luminosities (see K. Chiboucas et al. 2006, in preparation, for details). Simulations of spectra matching the instrumental resolution, signal-to-noise ratios, and spectral properties of our observational data showed that velocity dispersions below the instrumental resolution ($\log \sigma = 2.06$) may be subject to systematic errors as large as ± 0.15 in $\log \sigma$ (Jørgensen et al. 2005). Excluding from the analysis the four galaxies in the high-redshift sample with $\log \sigma < 2.06$, we find a slope for the M/L-mass relation of 0.47 ± 0.06, while the FP coefficients are not significantly different from those given in equation (2).

Finally, we address whether or not the selection effects can be the cause of the differences in the relations for the two samples. We choose 1000 random subsamples of 38 galaxies from the Coma sample, roughly matching the mass distribution of the high-redshift sample. We confirm the match in mass distributions by using a Kolmogorov-Smirnov test. The probability that the subsamples and the real high-redshift sample are drawn from the same parent distribution is above 90% for more than 90% of the realizations. For the remainder, the probability is above 70%. We then compare the fits to these subsamples to the results from bootstrapping the high-redshift sample. For the FP coefficients, the subsample fits overlap the bootstrap fits in only 1.6% of the cases (Fig. 2a), while for the M/L-mass relation, the slope for the subsamples overlaps the bootstrap fits in 3.7% of the cases (Fig. 2b). This shows that the FP and the M/L-mass relation for the high-redshift sample are different from the relations found for the Coma sample at the 96%–98% confidence level.

Based on the simulations of the data and the selection effects, we conclude that the differences in relations that we find between the Coma sample and the high-redshift sample are unlikely to be due to systematic effects in the data or due to differences in selection effects.

5. THE STAR FORMATION HISTORY OF E/S0 CLUSTER GALAXIES

The median offset of $\log (M/L)$ for the high-redshift sample relative to the Coma sample is -0.38. Using stellar population models from Maraston (2005), which show that $\Delta \log (M/L) = 0.935\Delta \log (\mathrm{age})$ (Jørgensen et al. 2005), this gives an epoch for the last major star formation episode of $z_{\mathrm{form}} \approx 3.2$. However, the steeper M/L-mass relation found for high-redshift clusters compared to the Coma Cluster may be due to a difference in the epoch of the last major star formation episode as a function of galaxy
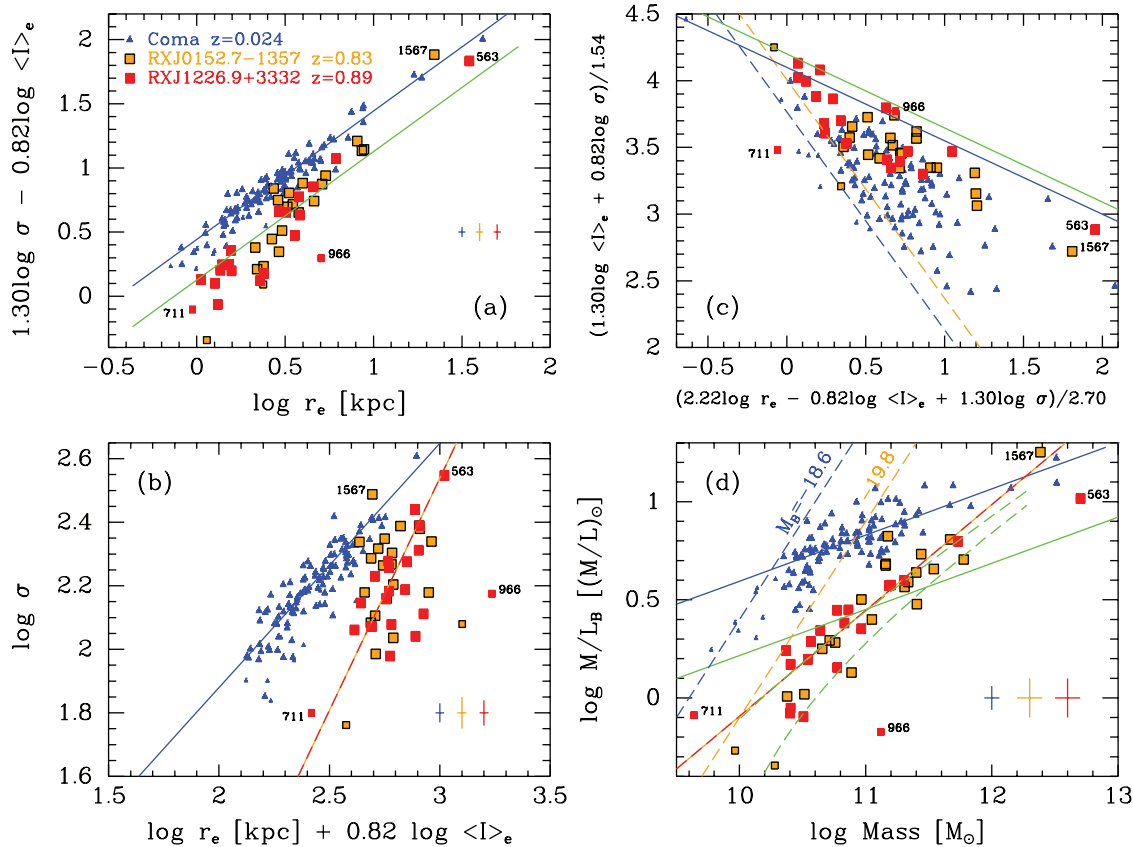
Fig. 1.—FP for RX J0152.7−1357 (*orange squares*), RX J1226.9+3332 (*red squares*), and Coma (*blue triangles*). The smaller symbols represent galaxies with $M < 10^{10.3}\ M_\odot$, excluded from the analysis. RX J1226.9+3332 ID = 711 and ID = 966 (with Sérsic index $n < 1.5$) are labeled and excluded from the analysis. (*a, b*) Edge-on view of the FP. (*c*) FP face-on, for the Coma Cluster coefficients. (*d*) FP as mass vs. *M/L*. The solid blue line in (*a*), (*b*), and (*d*) represents the fit to the Coma Cluster sample. The solid green line in (*a*) and (*d*) represents the Coma Cluster fit offset to the median zero point of the high-redshift sample. The orange-red line in (*b*) and (*d*) represents the fit to the high-redshift sample. The fit shown in (*b*) is not the optimal FP for the high-redshift sample since it has the coefficient for $\log \langle I \rangle_e$ fixed at 0.82. The dashed lines in (*c*) and (*d*) represent the luminosity limits for the Coma Cluster (*blue*) and both redshift clusters (*orange*). In (*c*) the solid blue and green lines mark the "exclusion zones" (Bender et al. 1992) for the Coma Cluster and high-redshift sample, respectively, assuming the slope and zero points as shown in (*a*). The dashed green lines in (*d*) represent models from Thomas et al. (2005; see text for discussion). Internal uncertainties are shown as representative error bars. In (*c*) the internal uncertainties are the size of the points.

mass. The low-mass galaxies have experienced the last major star formation episode much more recently than the high-mass galaxies. The difference between the high- and low-redshift samples is $\Delta \log (M/L) = -0.30 \log M + 3.72$, equivalent to $\Delta \log (\text{age}) = -0.32 \log M + 4.0$. Thus, for the lowest mass galaxies ($10^{10.3}\ M_\odot$), the last epoch of star formation may have been as recent as $z_{\text{form}} \approx 1.35$. This is only ≈ 1.5 Gyr prior to when the light that we now observe was emitted from the galaxies in the high-redshift sample. There appears to be just enough time for the galaxies to no longer have detectable emission lines due

to the massive stars formed at that time. Very shortly after the end of the last major star formation episode, these galaxies follow a tight FP. For galaxies with $M \approx 10^{10.8}\ M_\odot$, we find $z_{\text{form}} \approx 1.9$, while for galaxies with $M > 10^{11.3}\ M_\odot$, we find $z_{\text{form}} > 4.5$.

Thomas et al. (2005) used absorption-line index data for nearby E/S0 galaxies to establish rough star formation histories of the galaxies as a function of their masses. They find that the most massive galaxies form the majority of their stars at high redshift, while lower mass galaxies continue forming stars at much later epochs. Thomas et al. convert velocity dispersions to galaxy masses using a model-dependent relation that is inconsistent with our data. We therefore correct their masses to be consistent with our data by using the empirical relation between our mass estimates and the measured velocity dispersions. The lower of the two dashed green lines in Figure 1*d* shows the result based on the star formation history in high-density environments as established by Thomas et al. and on the *M/L* modeling from Maraston (2005). Our data show slightly less evolution in the *M/L* between $z \approx 0.8$–0.9 and the present than predicted by Thomas et al. However, it is striking that the slope of the predicted relation is in agreement with our data. As an experiment, we shifted the predictions from Thomas et al. to the best agreement with our data. The upper of the two dashed green lines shows this for the formation look-back times shifted 2.5 Gyr
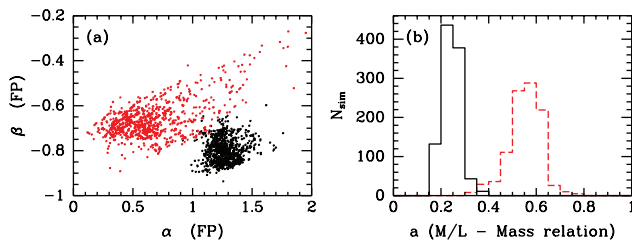

Fig. 2.—Distributions of FP coefficients and the slope, *a*, of the *M/L*-mass relation for 1000 subsamples of the Coma Cluster sample (*black points and histogram*) and for 1000 bootstrap samples of the high-redshift sample (*red points and histogram*). See text for discussion.

earlier for all masses such that the earliest formation look-back time is 14 Gyr (roughly the age of the universe in this cosmology). The absolute formation epochs from Thomas et al. may not be correct, since their analysis depends on stellar population models. However, their results on the relative timing of the star formation episodes as a function of galaxy mass closely match our results for this high-redshift sample.

Thomas et al. predict that star formation is ongoing for a longer period in low-mass galaxies than in high-mass galaxies. Based on this, we estimate that the internal scatter in the M/L-mass relation, in log (M/L), should be ≈ 0.06 at $10^{10.3}$ $M_\odot$ but only ≈ 0.01 at $10^{11.3}$ $M_\odot$. We cannot confirm such a decrease of the internal scatter. However, it would most likely require a larger sample and/or significantly smaller measurement uncertainties to test this prediction.

Factors other than the mean ages of the stellar populations could be affecting the M/L of the galaxies. For RX J0152.7−1357 we found, based on absorption-line index data, that a large fraction of the galaxies may have α-element abundance ratios, $[\alpha/\mathrm{Fe}]$, about 0.2 dex higher than found in nearby clusters (Jørgensen et al. 2005). This could affect the M/L in a systematic way. C. Maraston (2005, private communication) finds from modeling that stellar populations with $[\alpha/\mathrm{Fe}] = 0.3$, solar metallicities and ages of 2–7 Gyr may have M/L in the blue that are about 20% higher than those with $[\alpha/\mathrm{Fe}] = 0.0$. While it is still too early to use these models for a detailed analysis of high-redshift data, it indicates that for future detailed analysis of the FP, we may have to include information about the $[\alpha/\mathrm{Fe}]$ of the galaxies.

6. CONCLUSIONS

We find that the FP for E/S0 galaxies in the clusters RX J0152.7−1357 ($z = 0.83$) and RX J1226.9+3332 ($z = 0.89$)

is offset and rotated relative to the FP of our low-redshift comparison sample of Coma Cluster galaxies. Expressed as a relation between the M/L and the masses of the galaxies, the high-redshift galaxies follow a significantly steeper relation than found for the Coma Cluster. We interpret this as being due to a mass dependency of the epoch of the last major star formation episode. The lowest mass galaxies in the sample ($10^{10.3}$ $M_\odot$) have experienced significant star formation as recent as $z_{\mathrm{form}} \approx 1.35$, while high-mass galaxies ($M > 10^{11.3}$ $M_\odot$) have $z_{\mathrm{form}} > 4.5$. This is in general agreement with the predictions for the star formation histories of E/S0 galaxies from Thomas et al. (2005) based on their analysis of line index data for nearby galaxies. The scatter of FP for these two $z = 0.8$–0.9 clusters is as low as found for the Coma Cluster, and we find no significant difference in the scatter for low- and high-mass galaxies. This indicates that at a given galaxy mass, the star formation history for the E/S0 galaxies is quite similar. In a future paper we will discuss these results in connection with our absorption-line index data for the galaxies in both high-redshift clusters.

REFERENCES

Bender, R., Burstein, D., & Faber, S. M. 1992, ApJ, 399, 462
Bernardi, M., et al. 2003, AJ, 125, 1866
Blakeslee, J. P., Lucey, J. R., Tonry, J. L., Hudson, M. J., Narayanan, V. K., & Barris, B. J. 2002, MNRAS, 330, 443
Claver, C. F. 1995, Ph.D. thesis, Univ. Texas
Colless, M., Saglia, R. P., Burstein D., Davies, R. L., McMahan Jr., R. K., & Wegner, G. 2001, MNRAS, 321, 277
de Lucia, G., et al. 2004, ApJ, 610, L77
di Serego Alighieri, S., et al. 2005, A&A, 442, 125
Djorgovski, S., & Davis, M. 1987, ApJ, 313, 59
Dressler, A., Lynden-Bell, D., Burstein, D., Davies, R. L., Faber, S. M., Terlevich, R., & Wegner G. 1987, ApJ, 313, 42
Gebhardt, K., et al. 2003, ApJ, 597, 239
Holden, B. P., et al. 2005, ApJ, 620, L83
Hook, I. M., Jørgensen, I., Allington-Smith, J. R., Davies, R. L., Metcalfe, N., Murowinski, R. G., & Crampton, D. 2004, PASP, 116, 425
Jørgensen, I. 1999, MNRAS, 306, 607
Jørgensen, I., Bergmann, M., Davies, R., Jordi, B., Takamiya, M., & Crampton, D. 2005, AJ, 129, 1249
Jørgensen, I., Franx, M., Hjorth, J., & van Dokkum, P. G. 1999, MNRAS, 308, 833

Jørgensen I., Franx, M., & Kjærgaard, P. 1995, MNRAS, 273, 1097
———. 1996, MNRAS, 280, 167 (JFK1996)
Kelson, D. D., Illingworth, G. D., van Dokkum, P. G., & Franx, M. 2000, ApJ, 531, 184
Maraston, C. 2005, MNRAS, 362, 799
Peng, C. Y., Ho, L. C., Impey, C. D., & Rix, H.-W. 2002, AJ, 124, 266
Sérsic, J. L. 1968, Atlas de Galaxias Australes (Córdoba: Obs. Astron. Univ. Nac. Córdoba)
Thomas, D., Maraston, C., Bender, R., & de Oliveira, C. M. 2005, ApJ, 621, 673
Toft, S., Mainieri, V., Rosati, P., Lidman, C., Demarco, R., Nonino, M., & Stanford, S. A. 2004, A&A, 422, 29
Treu, T., et al. 2005, ApJ, 633, 174
van der Wel, A., Franx, M., van Dokkum, P. G., Rix, H.-W., Illingworth, G. D., & Rosati, P. 2005, ApJ, 631, 145
van de Ven, G., van Dokkum, P. G., & Franx, M. 2003, MNRAS, 344, 924
Wuyts, S., van Dokkum, P. G., Kelson, D. D., Franx, M., & Illingworth, G. D. 2004, ApJ, 605, 677
Ziegler, B. L., Thomas, D., Böhm, A., Bender, B., Fritz, A., & Maraston, C. 2005, A&A, 433, 519

ERRATUM: "THE FUNDAMENTAL PLANE FOR $z = 0.8$–0.9 CLUSTER GALAXIES" (ApJ 639, L9 [2006])

INGER JØRGENSEN, KRISTIN CHIBOUCAS, KATHLEEN FLINT, MARCEL BERGMANN, JORDI BARR, AND ROGER DAVIES

In the above-mentioned Letter, an incorrect calibration of the photometry to the rest-frame B band was used for the two high-redshift clusters RX J0152.7$-$1357 ($z = 0.83$) and RX J1226.9$+$3332 ($z = 0.89$). This error was identified with the help of P. van Dokkum. To correct for the error, the photometry for the two high-redshift clusters should be offset to brighter luminosities with a factor $(1 + z_{\mathrm{cluster}})$, corresponding to an average offset in $\log L$ for the two clusters of $\log (1 + 0.86) = 0.27$.

With this error corrected, the fundamental plane (FP) for the two high-redshift clusters (eq. [2] in the above-mentioned Letter) should read

$$\log r_e = (0.60 \pm 0.22) \log \sigma - (0.70 \pm 0.06) \log \langle I \rangle_e + 1.32. \tag{1}$$

The relation between the galaxy masses and the mass-to-light ratio (eq. [4] in the above-mentioned Letter) should read

$$\log (M/L) = (0.54 \pm 0.08) \log M - 5.74. \tag{2}$$

We include a revised version of Figure 1 that reflects these changes.

The discussion of the possible systematic effects and the simulations supporting the conclusion that the FP is steeper for the high-redshift sample compared to that of the Coma Cluster remain unchanged (§ 4 and Fig. 2 of the above-mentioned Letter).

The offsets and relations stated in § 5 in the above-mentioned Letter change as follows. The median offset of $\log (M/L)$ for the high-redshift sample relative to the Coma sample is -0.65, corresponding to an epoch of the last major star formation episode of $z_{\mathrm{form}} \approx 1.3$. The mass-dependent difference in $\log (M/L)$ between the high- and low-redshift samples is $\Delta \log (M/L) = -0.30 \log M + 3.99$, equivalent to $\Delta \log (\mathrm{age}) = -0.32 \log M + 4.27$. Thus, for the lowest mass galaxies ($10^{10.3} M_{\odot}$), the last epoch of star formation may have been as recent as $z_{\mathrm{form}} \approx 1.1$. This is only ≈ 1 Gyr prior to when the light that we now observe was emitted from the galaxies in the high-redshift sample. For galaxies with $M \approx 10^{10.8} M_{\odot}$, we find $z_{\mathrm{form}} \approx 1.25$, while for galaxies with $M > 10^{11.3} M_{\odot}$, we find $z_{\mathrm{form}} \gtrsim 1.6$.

As the revised Figure 1 shows, the predictions from Thomas et al. (2005) are in quite good agreement with our high-redshift data, and no offset to higher look-back times is needed.

The remainder of the above-mentioned Letter is unaffected by the error in the calibration. The authors regret the mistake and thank P. van Dokkum for assisting in identifying this problem.
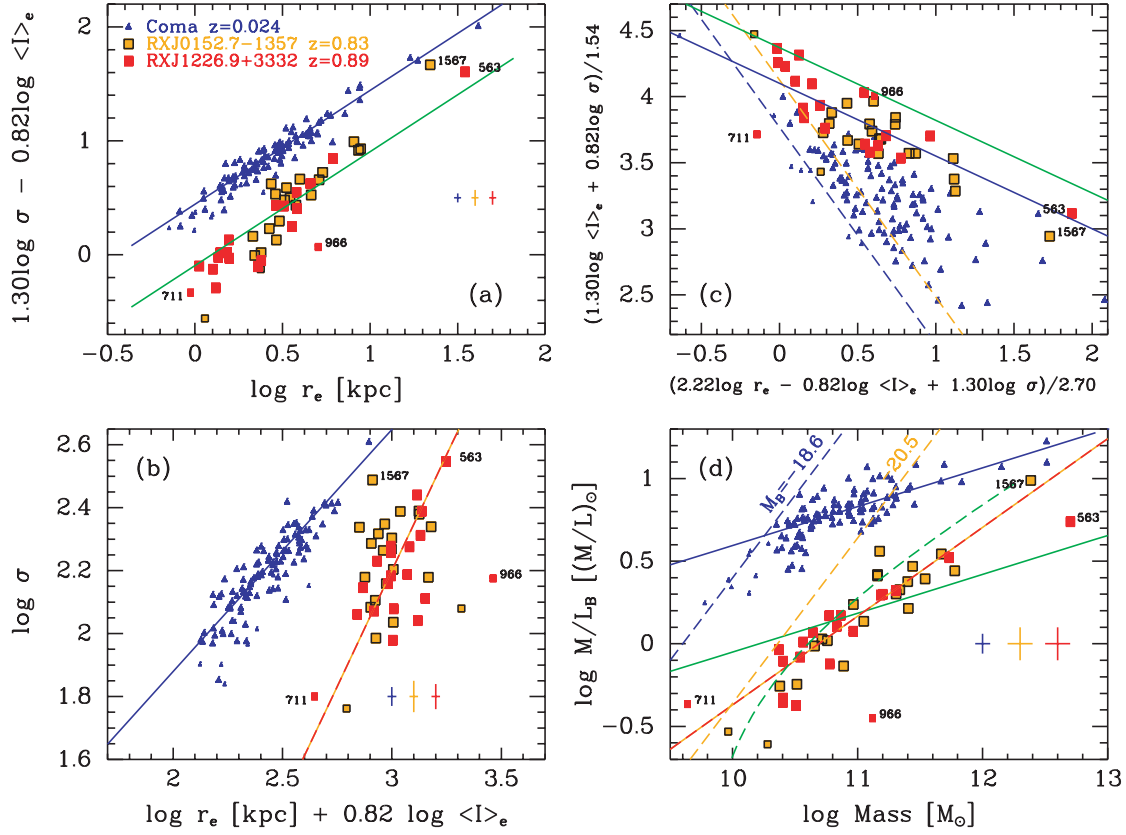
Fɪɢ. 1.—FP for RX J0152.7−0152 (*orange squares*), RX J1226.9+3332 (*red squares*), and Coma (*blue triangles*). The smaller symbols represent galaxies with $M < 10^{10.3} M_\odot$, excluded from the analysis. RX J1226.9+3332 ID = 711 and ID = 966 (with Sérsic index $n < 1.5$) are labeled and excluded from the analysis. (*a, b*) Edge-on view of the FP. (*c*) FP face-on, for the Coma Cluster coefficients. (*d*) FP as Mass vs. *M/L*. The solid blue line in (*a*), (*b*), and (*d*) represent the fit to the Coma Cluster sample. Solid green line in (*a*) and (*d*) represent the Coma Cluster fit offset to the median zero point of the high-redshift sample. Orange-red line in (*b*) and (*d*) represent the fit to the high-redshift sample. The fit shown in (*b*) is not the optimal FP for the high-redshift sample since it has the coefficient for log ⟨*I*⟩ₑ fixed at 0.82. The dashed lines in (*c*) and (*d*) represent the luminosity limits for the Coma Cluster (*blue*) and both redshift clusters (*orange*). In (*c*) the solid blue and green lines mark the "exclusion zones" (Bender et al. 1992) for the Coma Cluster and high-redshift sample, respectively, assuming the slope and zero points as shown in (*a*). The dashed green line in (*d*) represents the model from Thomas et al. (2005; see text for discussion). Internal uncertainties are shown as representative error bars. In (*c*) the internal uncertainties are the size of the points.